CHAPTER C.3
HYDRODYNAMIC MODELS OF SUBPROVINCE 1

J. Alex McCorquodale[1]
Ioannis Georgiou[2]

[1] *Department of Civil and Environmental Engineering, University of New Orleans, New Orleans, LA 70148*
[2] *Pontchartrain Institute for Environmental Sciences, University of New Orleans, New Orleans, LA 70148*

3.1 Introduction

In coastal Louisiana, the growing restoration efforts have focused on the need for the re-introduction of freshwater and sediment from the Mississippi River to the endangered wetlands. Given the immense wetland loss over the past 100 years, multiple high flow diversions are being considered as a strategy for coastal rehabilitation. For the purposes of analyses the coastal region has been divided in to four subprovinces. The Pontchartrain Estuary is referred to as Subprovince 1. The estuary has been further sub-divided into: Upper (Maurepas), Middle (Lake Pontchartrain), and Lower (Lake Borgne and Breton Sound), shown in Figure C.3-1 and 3-2. The purpose of this sub-division was to permit better generalization of the results.

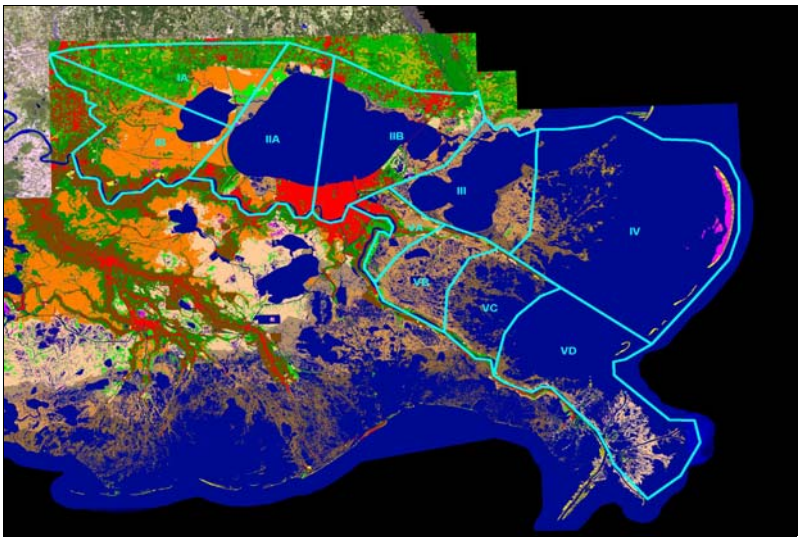

Figure C.3-1 Example of Box Distribution and Boundaries in Subprovince 1

Figure C.3-2 Location of Subprovince 1 Study Area, Including Estuary Subdivisions

Several possible locations for diversion opportunities have been identified by CWWPRA within Subprovince 1. Some of the possible diversion sites include:

1. The Bonnet Carré Spillway, a floodway structure that diverts floodwater from the Mississippi River into Lake Pontchartrain. (Middle Estuary)
2. Hope Canal, a man-made canal leading to the Amite/Blind River System then into Lake Maurepas. (Upper Estuary)
3. Caernarvon, an existing freshwater diversion structure, located at approximately Mile 81.5. (Lower Estuary), and California bay, Whites Ditch, and Bayou Lamoque.

3.2 Model Objectives

The hydrodynamic modeling of Subprovince 1 had three main objectives. The first objective was to model the hydrologic and salinity regime changes that various diversions would cause relative to a base condition. The second objective was to provide indicators of the relative impact of the various diversion options on the water quality in the Subprovince 1 estuary. The third objective was to use the model results to assist in the preparation of habitat impacts on selected sub-regions of Subprovince 1.

3.3 Methods

The Princeton Ocean Model (POM) was used for this study. This model was developed by Blumberg and Mellor (1987) at Princeton University. It is a public domain model with a very

active user's group. It has been applied in oceans, lakes, and estuaries. The POM bathometry was almost doubled to include the area between the mouth of the Mississippi and Gulfport by adding bathometry from other working models. However, data were only available for validation for the Lake Pontchartrain area.

POM is a free surface three-dimensional sigma coordinate primitive variable model. The model solves the continuity and momentum equations (Eq. 1, 2, and 3) and the transport equation for temperature and salinity (Eq. 4). The temperature and salinity transport is coupled to velocity through the equation of state relationship. The model also incorporates a 2.5-level turbulence closure scheme to provide vertical mixing coefficients (Mellor and Yamada 1982) and horizontal mixing is accomplished by the Smagorinsky formulation (Eq. 7). The generic form of the transport equation is given as Eq. 8.

$$[1]\ \frac{\partial DU}{\partial x}+\frac{\partial DV}{\partial y}+\frac{\partial \omega}{\partial \sigma}+\frac{\partial \eta}{\partial t}=0$$

$$[2]\ \frac{\partial UD}{\partial t}+\frac{\partial U^2 D}{\partial x}+\frac{\partial UVD}{\partial y}+\frac{\partial U\omega}{\partial \sigma}-fVD+gD\frac{\partial \eta}{\partial x}$$
$$+\frac{gD^2}{\rho_o}\int_\sigma^o\left[\frac{\partial \rho'}{\partial x}-\frac{\sigma'}{D}\frac{\partial D}{\partial x}\frac{\partial \rho'}{\partial \sigma'}\right]d\sigma'=\frac{\partial}{\partial \sigma}\left[\frac{K_M}{D}\frac{\partial U}{\partial \sigma}\right]+F_x$$

$$[3]\ \frac{\partial VD}{\partial t}+\frac{\partial UVD}{\partial x}+\frac{\partial V^2 D}{\partial y}+\frac{\partial V\omega}{\partial \sigma}+fUD+gD\frac{\partial \eta}{\partial y}$$
$$+\frac{gD2}{\rho_o}\int_\sigma^o\left[\frac{\partial \rho'}{\partial y}-\frac{\sigma'}{D}\frac{\partial D}{\partial y}\frac{\partial \rho'}{\partial \sigma'}\right]d\sigma'=\frac{\partial}{\partial \sigma}\left[\frac{K_M}{D}\frac{\partial V}{\partial \sigma}\right]+F_y$$

The horizontal viscosity and diffusion terms are defined according to:

$$[4]\ F_x\equiv\frac{\partial}{\partial x}\left(H\tau_{xx}\right)+\frac{\partial}{\partial y}\left(H\tau_{xy}\right)$$

$$[5]\ F_y\equiv\frac{\partial}{\partial x}\left(H\tau_{xy}\right)+\frac{\partial}{\partial y}\left(H\tau_{yy}\right)$$

where,

$$[6]\ \tau_{xx}=2A_M\frac{\partial U}{\partial x},\ \tau_{xy}=\tau_{yx}=A_M\left(\frac{\partial U}{\partial y}+\frac{\partial V}{\partial x}\right),\ \tau_{yy}=2A_M\frac{\partial V}{\partial y}$$

$$[7]\ A_M=C\Delta x\Delta y\frac{1}{2}\left|\nabla\mathbf{V}+(\nabla\mathbf{V})^T\right|$$

where $|\nabla \mathbf{V} + (\nabla \mathbf{V})^{\mathrm{T}}| /2 = [(\partial u / \partial x)^2 + (\partial v / \partial x + \partial u / \partial y)^2 / 2 + (\partial v / \partial y)^2]^{1/2}$.

The generic form of the transport equation is shown as Eq. 8,

[8] $$\frac{\partial \varphi D}{\partial t} + \frac{\partial \varphi UD}{\partial x} + \frac{\partial \varphi VD}{\partial y} + \frac{\partial \varphi W}{\partial \sigma} = \frac{\partial}{\partial \sigma}\left[\frac{K_H}{D}\frac{\partial \varphi}{\partial \sigma}\right] + F_\varphi$$

where φ is the transportable variable; *U, V, W* are the horizontal and vertical velocity components; *x, y, σ, t* are the independent variables representing horizontal and vertical space and time; *D* is the depth of the water column; K_H is the vertical diffusion coefficient, and F_φ are the horizontal viscosity and diffusion terms.

The model formulation uses the finite control volume principle. The model has a two-time step solution scheme. The horizontal (external) free surface mode solves the depth-average surface wave equation using a small time step. The internal mode solves the three-dimensional part using a much larger time step of the order of 50 times the external time step. It is a three time level model and time stepping is accomplished by the leapfrog scheme. The reader is referred to Blumberg and Mellor 1987 for more details regarding the model equations and solution schemes.

3.4 Model Development

The model computational grid and bathymetry is shown in Figure C.3-3. The model has 11-sigma layers with logarithmic spacing near the surface. The grid size varies from 657.17 ft (200 m) (upper basin, Lake Maurepas) to 3,280 ft (1 km) (Gulf of Mexico).

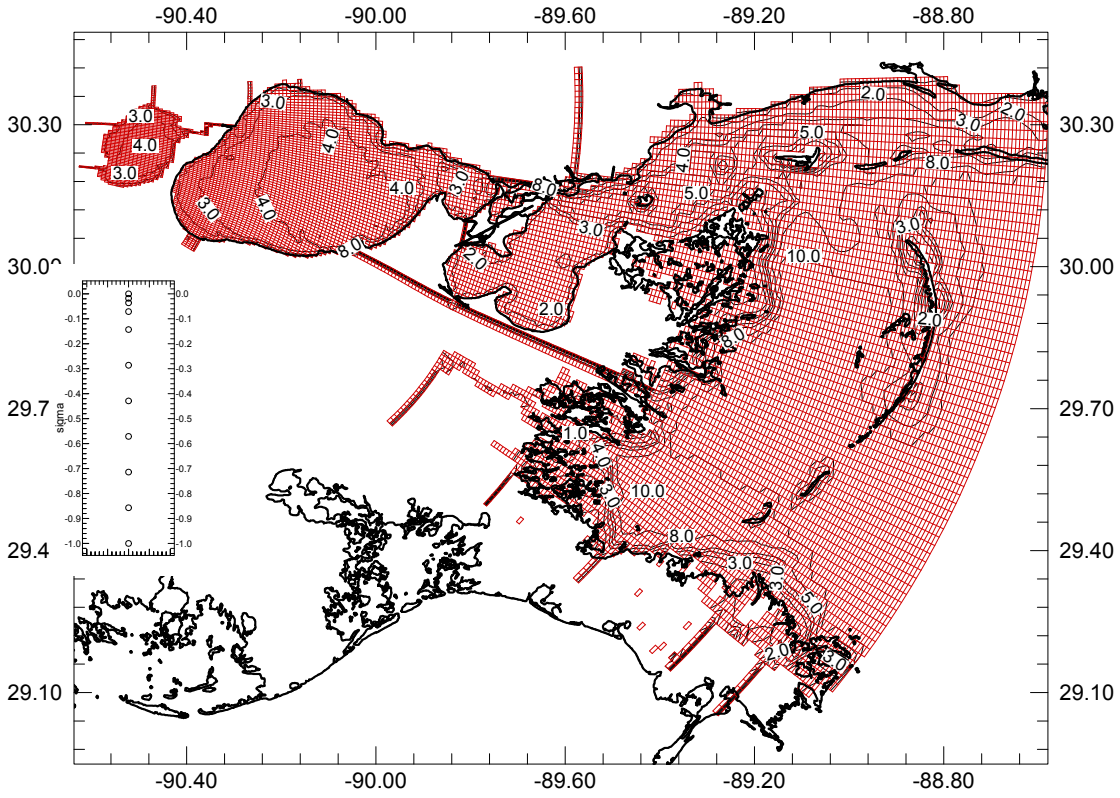

Insert shows the vertical segmentation as a percentage of the water column.

Figure C.3-3 Model Computational Domain and Bathymetry

A sub-model for dissolved inorganic nitrogen (DIN) was incorporated in the model to assess the potential triggering of algal blooms in the system. DIN transport was achieved through the 3D advection-diffusion equation. Following the transport, DIN concentrations were corrected for decay. Field data from the 1997 Bonnet Carré spillway suggested that DIN die-off follows second order kinetics. Thus, a multiple decay first-order kinetics equation was applied as a correction to the concentration obtained by the transport equation in the model. This resulted in two inactivation k constants (for high and low nitrogen concentrations), as well as relationships relating the DIN inactivation constants to the depth of the water column. The combined effects were incorporated into one k value, and Eq. 9 was used for the decay calculation at each time step.

$$[9]\quad C = (C_o - C_b)(1 - \Delta t \cdot k) + C_b$$

where, k is the composite inactivation constant [h^{-1}]; C_o is the transported DIN concentration prior to decay [mg/L]; C is the corrected concentration including decay [mg/L]; C_b is the background pathogen concentration for the lake [MPN/100 mL]; Δt is the model time step [h].

3.5 Boundary Conditions

Velocity boundary conditions were applied at all the tributaries and proposed diversion structures. The obtained flow from a hydrograph was converted to velocity internally in the model on daily basis. Tributary flows were obtained from USGS stations. The mean daily flow for each day was averaged over a 10-year period (1990 – 2000) and was stored in memory for each run (Figure C.3-4). Similarly, diversion hydrographs were available as mean monthly flows (Figure C.3-5 – 3-8). The shoreline boundaries were treated as solid walls with a half-slip condition, except where the tributary flows are introduced, in which case the longitudinal velocity component was considered. At the eastern boundary, an internal tide function was used to generate tidal elevations across the boundary throughout the year with three harmonic constituents and an initial surge option. Tidal lag times across the eastern boundary were also considered by adjusting the elevation to offset the "time before high water".

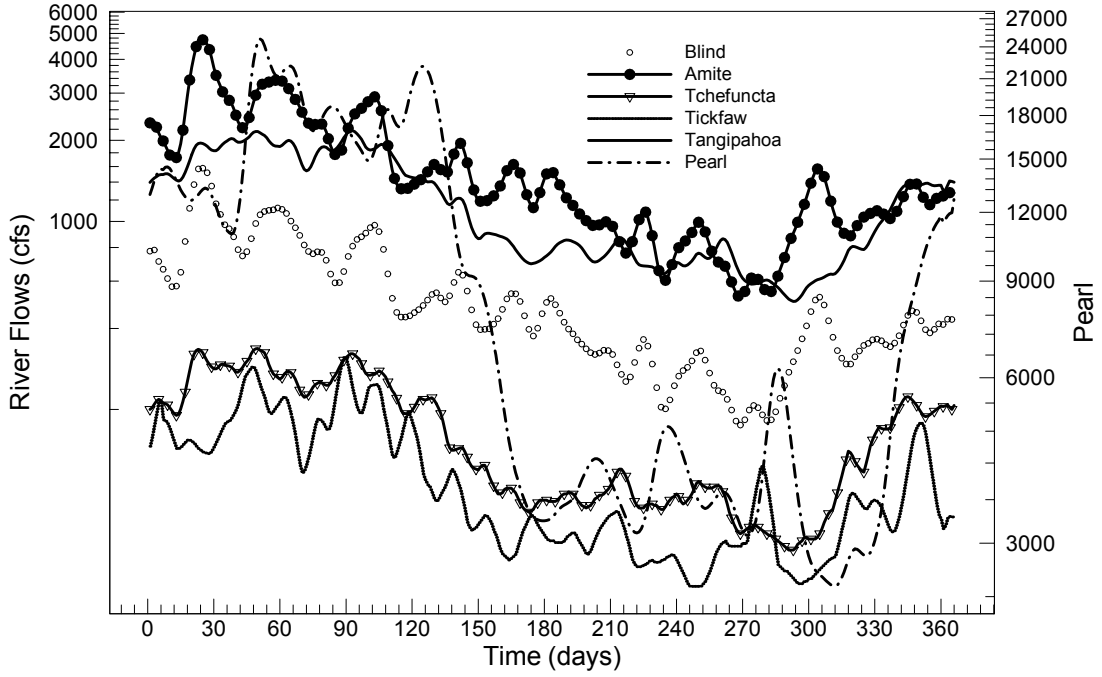

Flows are a 10 year average of the mean daily flow.

Figure C.3-4 Tributary flows used in POM

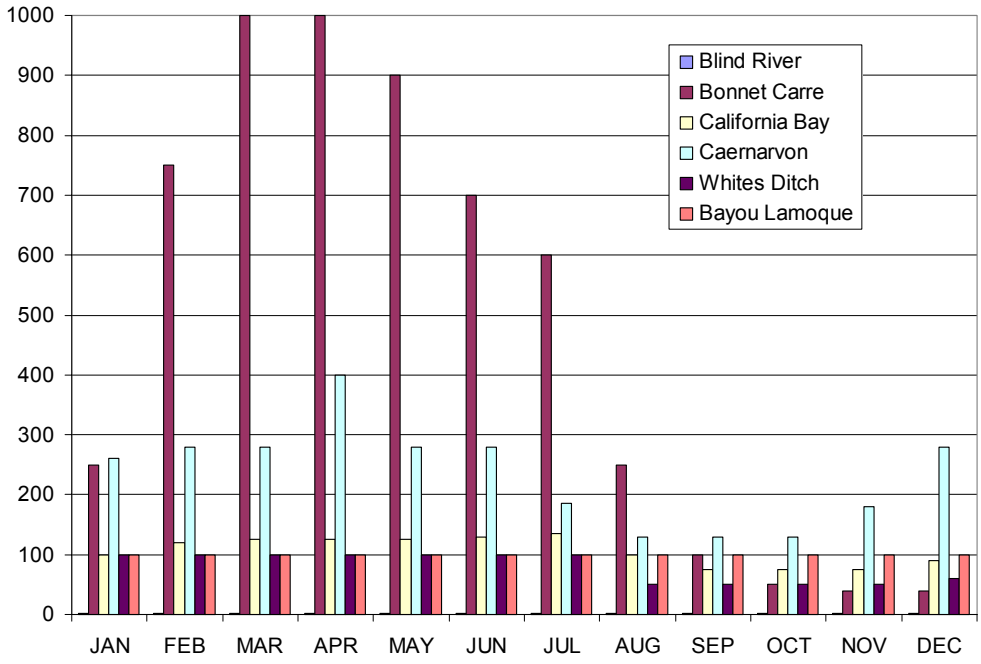

Figure C.3-5 Diversion Hydrograph for the Base Alternative

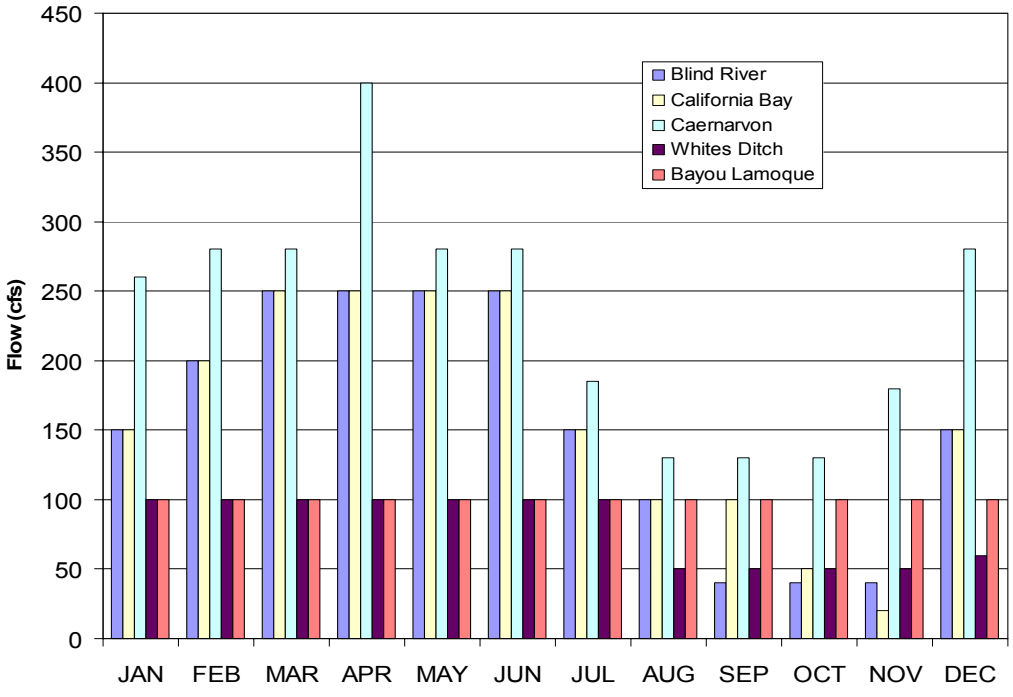

Bonnet Carré flow is constant at 5,000 cfs (not shown on figure)

Figure C.3-6 Diversion Hydrograph for the Reduce alternative

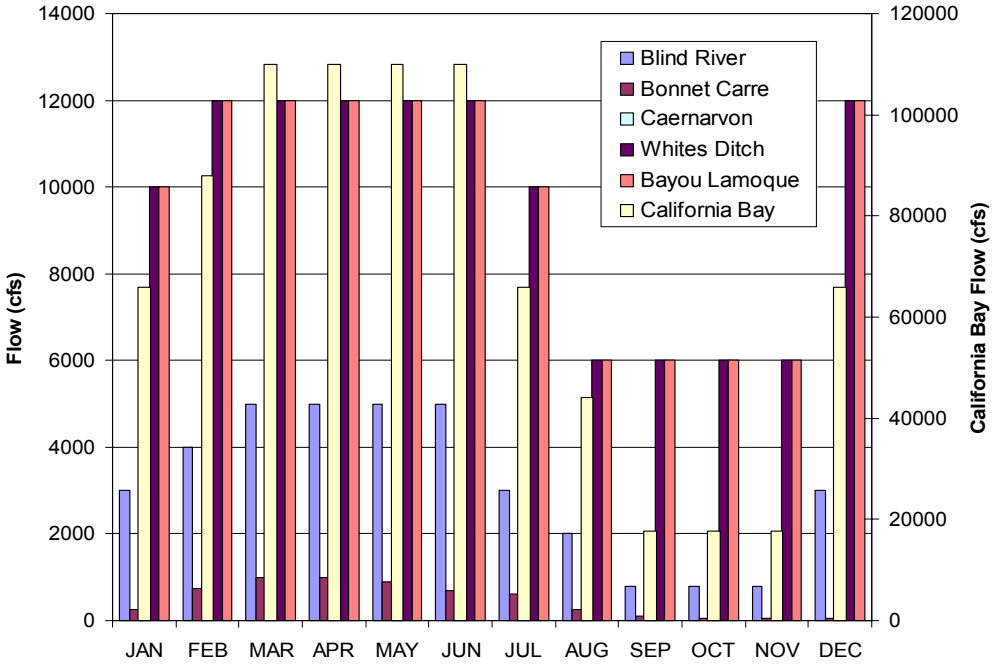

Figure C.3-7 Diversion Hydrograph for the Maintain Alternative

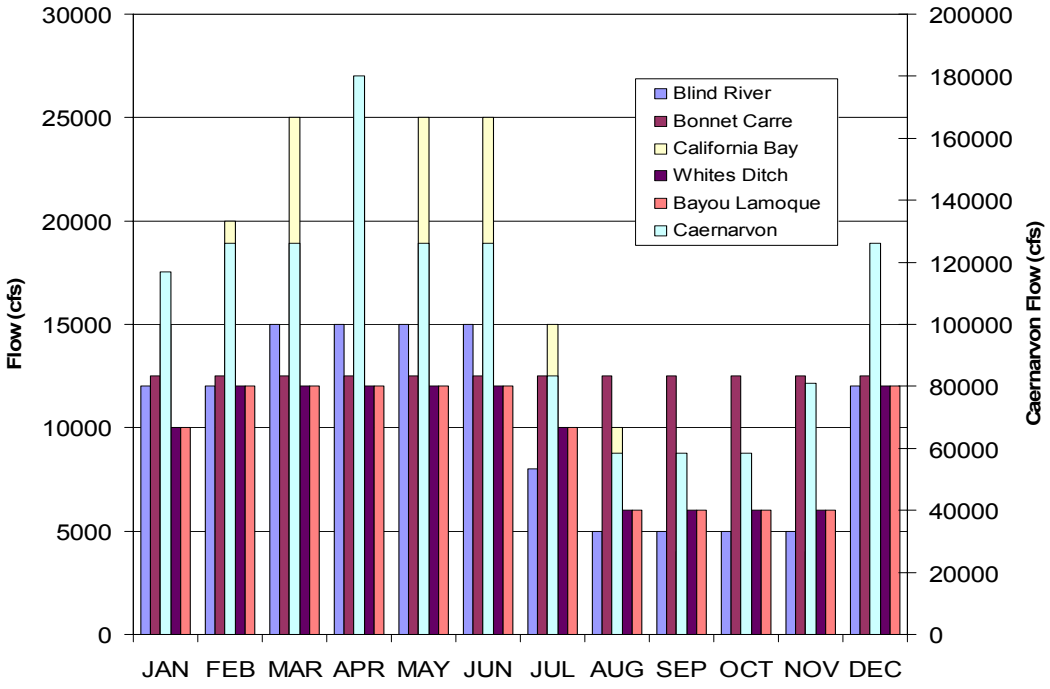

Figure C.3-8 Diversion Hydrograph for the Enhanced Alternative

Wind forcing in the model was achieved by applying wind shear near the water surface. Mid-lake hourly wind data were selected and averaged over a six-hour period to remove peaks in the signal. Wind shear was assumed uniform in space and was furthermore damped near the coastal boundary to avoid oscillations, and it was set to zero in channels, passes and in the marshes to avoid drying.

Precipitation and evapotranspiration were included in the model as a net increase or decrease of flow at the nearest tributary inflow boundary. The net flow was calculated using data from evaporation studies for Lake Pontchartrain, based on a segment of the local basin area.

3.6 Calibration and Verification

The POM was calibrated for Lake Pontchartrain and Maurepas (Georgiou 2002). Figure C.3-9 shows a time series comparison of observed and modeled data. POM appears to slightly under- predict the observed elevation. This is partially due to the assumed tidal elevation at the Inner Harbor Navigation Canal (IHNC) in the absence of data, which might influence the elevation gauge predictions at the mid-lake station. However, the overall agreement was good with a correlation coefficient of 0.96, and a root mean square error of less than 10 percent (Table C.3-1). Table C.3-2 shows observed and modeled surface currents under both fair and frontal weather conditions. The model captures the surface currents with a 96 percent agreement for the mean velocity and 93 percent agreement for the root mean square velocity.

The grid used for this study was not fully calibrated. The transport component was verified with available data in the Caernarvon Basin. No velocity or water surface elevations were available for calibration in the open water areas near the Gulf of Mexico, such as Breton Sound and Chandeleur Sound. The model, however, behaves similarly with typical observations of longshore and mid-lake currents, water surface elevations fluctuations and transport in the upper basin. The model also correctly captures wind induced circulation in all enclosed lakes (Lake Pontchartrain, Maurepas, and Borgne), consistent with field data and other numerical studies.

It is important to note that the model was not calibrated for large flows through a channel, such as the ones presented in this document. Data from such large flows are generally unavailable. Furthermore, there is an error associated with large flows restricted through a non-eroding channel as POM does not have wetting and drying, or sediment transport. These model limitations are being evaluated in several research projects that have been funded to improve model development for coastal restoration. A subroutine for wetting and drying wetlands coupled with forcings from coastal channels has been developed on another research project looking at wetland hydrology (Meselhe and Twilley, unpublished).

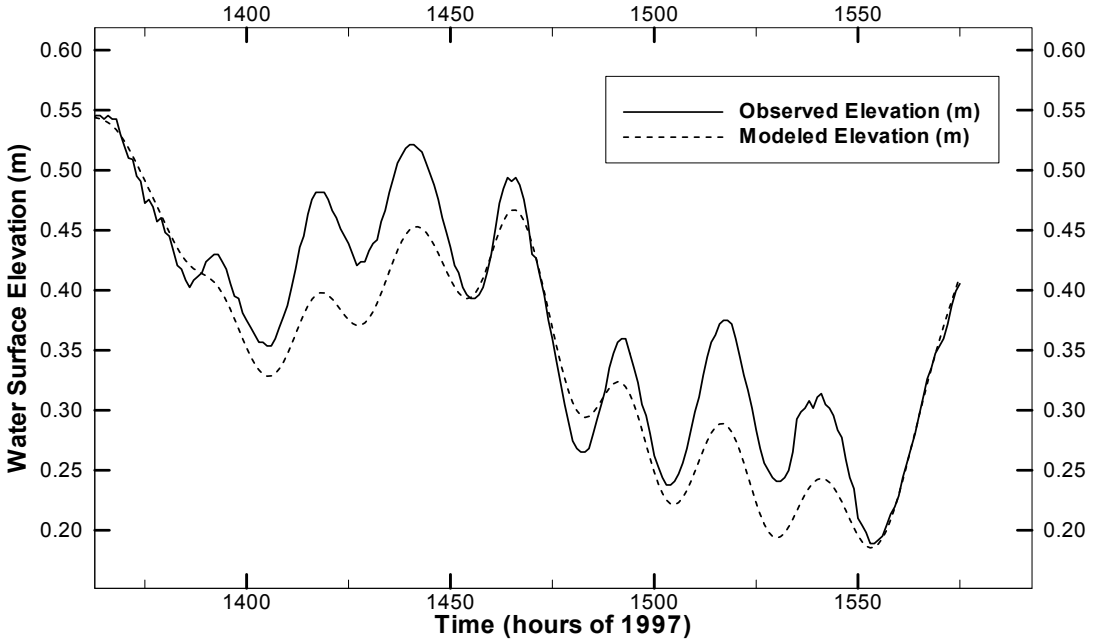

Figure C.3-9 Observed and Modeled Water Surface Elevation at the Mid lake Station in Lake Pontchartrain

Table C.3-1 Error analysis for POM in Lake Pontchartrain.

Observed mean (m)	Modeled mean (m)	Mean absolute	Root-mean-square error (m)	Observed change (m)	Relative root-mean-square error (%)
0.403	0.373	0.0258	0.0413	0.4633	8.89

Table C.3.-2 Observed and Modeled Currents in Lake Pontchartrain

Event Date	Mean Velocity (cm/s)	Min Velocity (cm/s)	Max Velocity (cm/s)	RMS Velocity (cm/s)	Mean Wind Speed (m/s)	Primary Direction
Oct 7 2000 (Obs)	5.97	1.48	15.71	4.14	4.50	N
Model	6.23	1.65	16.50	3.85	5.00	
July 19 2001 (Obs)	7.89	1.40	27.49	3.15	4.25	WSW
Model	7.36	1.73	14.00	2.95	5.00	
July 26 2001 (Obs)	6.42	1.22	52.07	1.35	3.67	SSE
Sept 19 2001 (Obs)	5.33	0.92	17.80	1.42	3.10	SSE
Model	5.85	1.52	13.52	1.30	5.00	

* *Velocities were calculated from GPS drifter deployments near the south shore during another study.*

3.7 Results (Base and Optimized Plan)

Results from the numerical model are shown in Figure C.3-10 – 3-13. These are static images (snapshots) of typical salinity distribution around mid-April for all the simulation alternatives including Base, Reduce, Maintain and Enhanced. In addition, seasonal trends are shown in Figure C.3-14 – 3-17 for each scenario. The salinity values shown are the monthly means from the selected sub-divisions of the Subprovince basin. As previously mentioned, this was done for easy comparisons between each alternative.

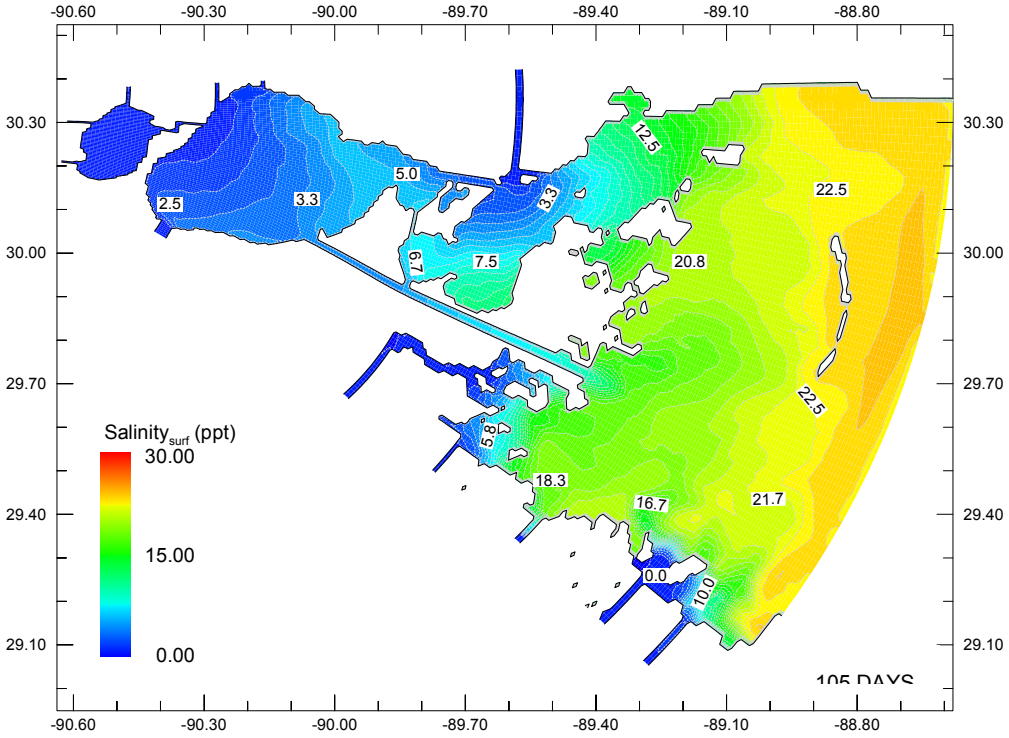

Figure C.3-10 Surface Salinity Distribution for Mid-April from the Future Without Scenario

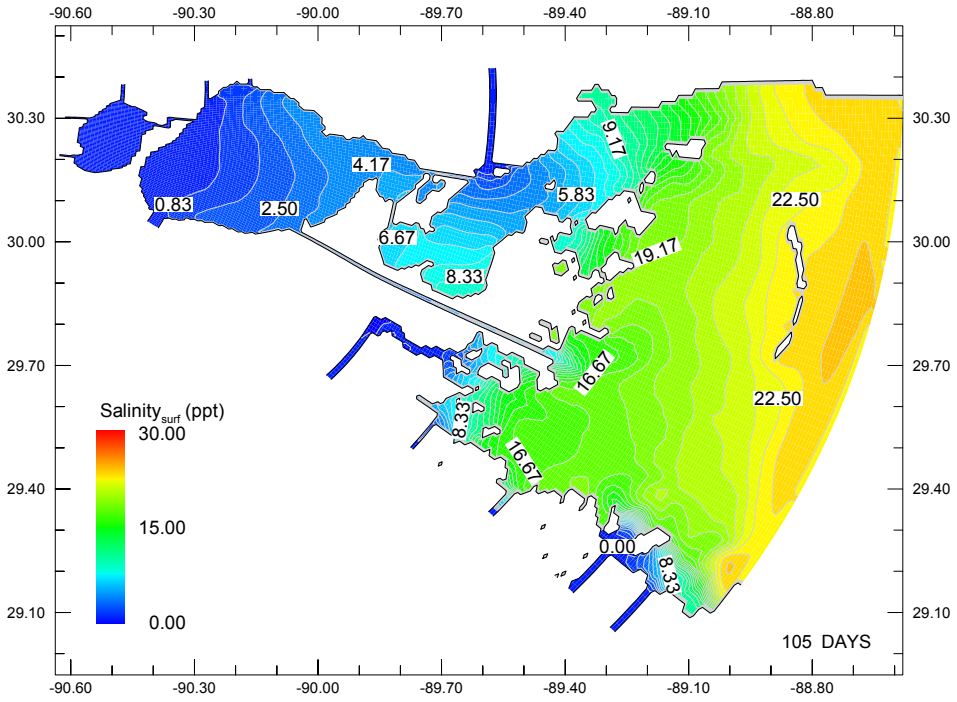

Figure C.3-11 Surface Salinity Distribution for Mid-April from the Reduce Alternative

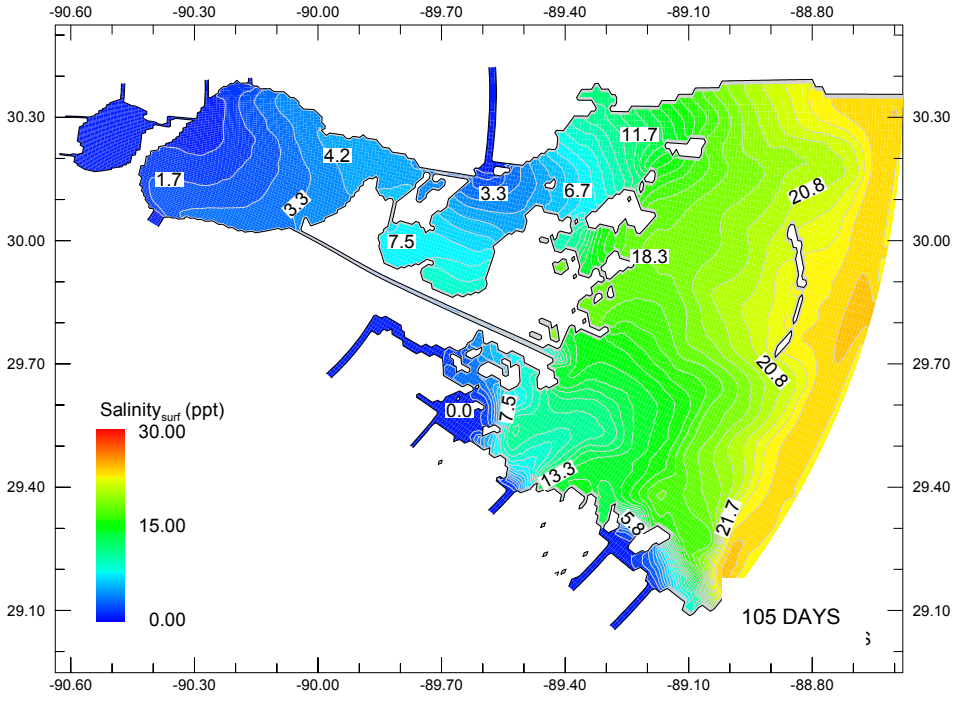

Figure C.3-12 Surface Salinity Distribution for Mid-April from the Maintain Alternative

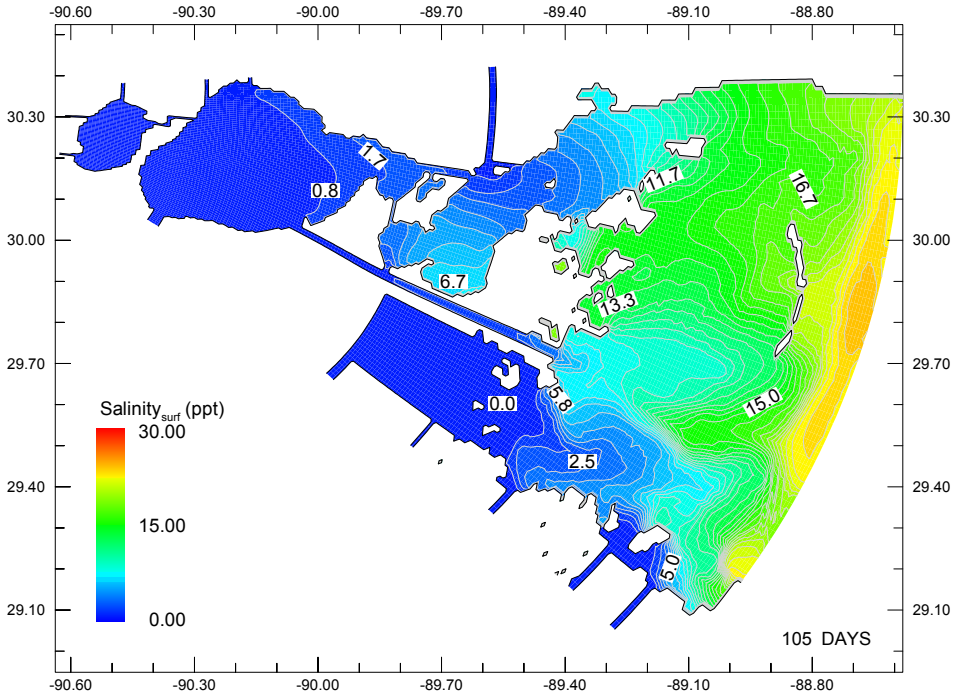

Figure C.3-13 Surface Salinity Distribution for Mid-April from the Enhanced Alternative

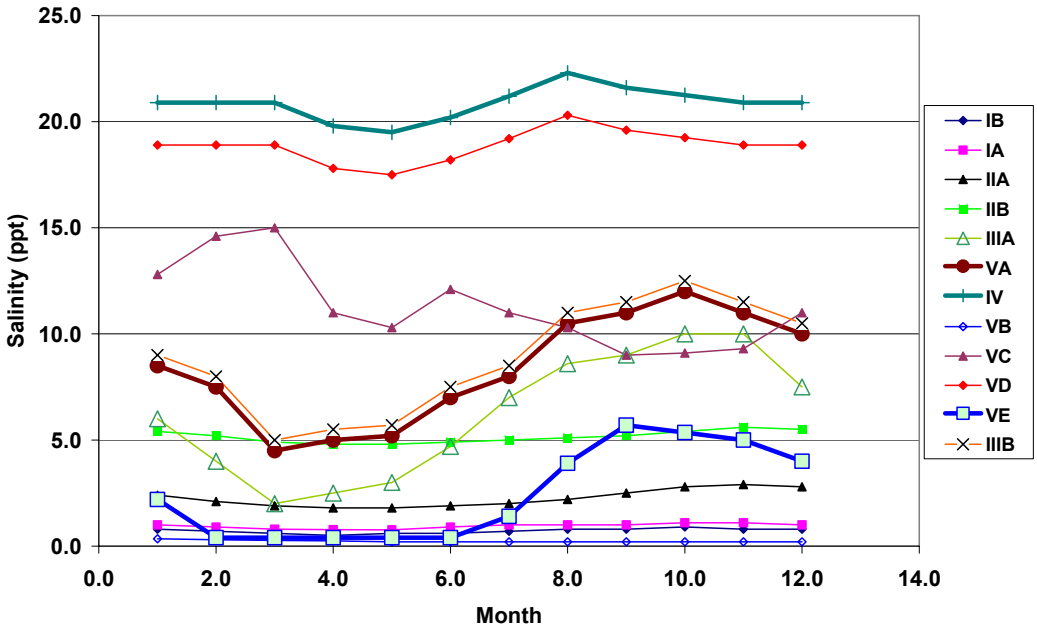

(stations are means for boxes as identified in Figure C.3-1)

Figure C.3-14 Monthly Mean Salinity for Future Without Alternative, Subprovince 1.

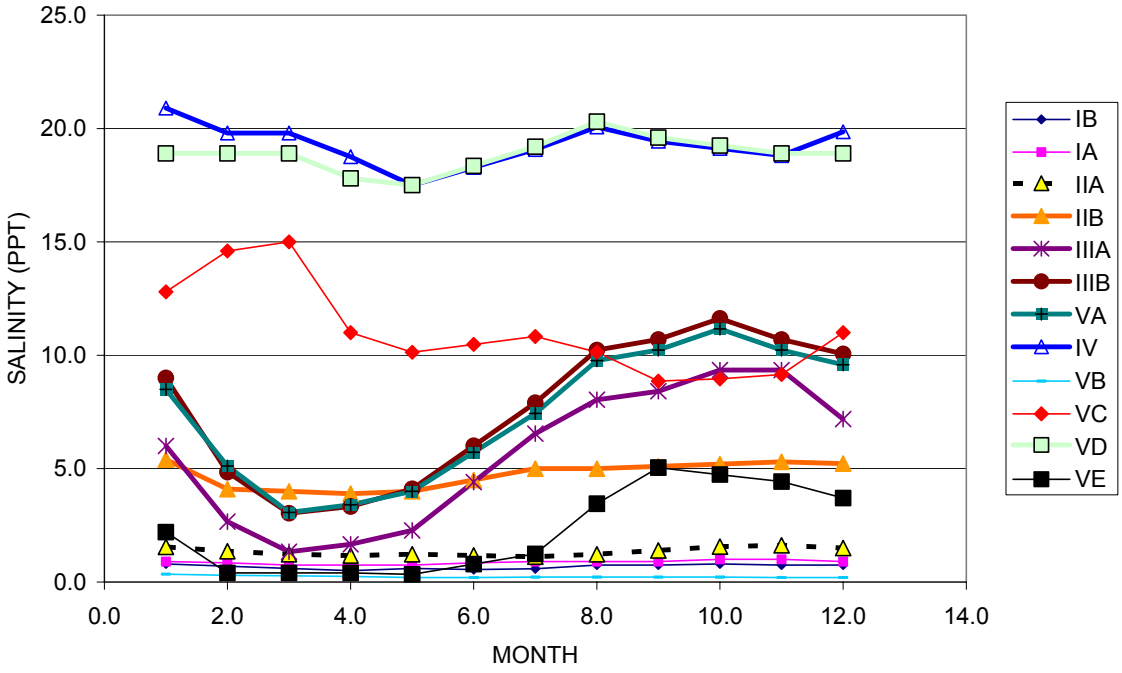

(stations are means for boxes as identified in Figure C.3-1)

Figure C.3-15 Monthly Mean Salinity for the Reduced Alternative, Subprovince 1.

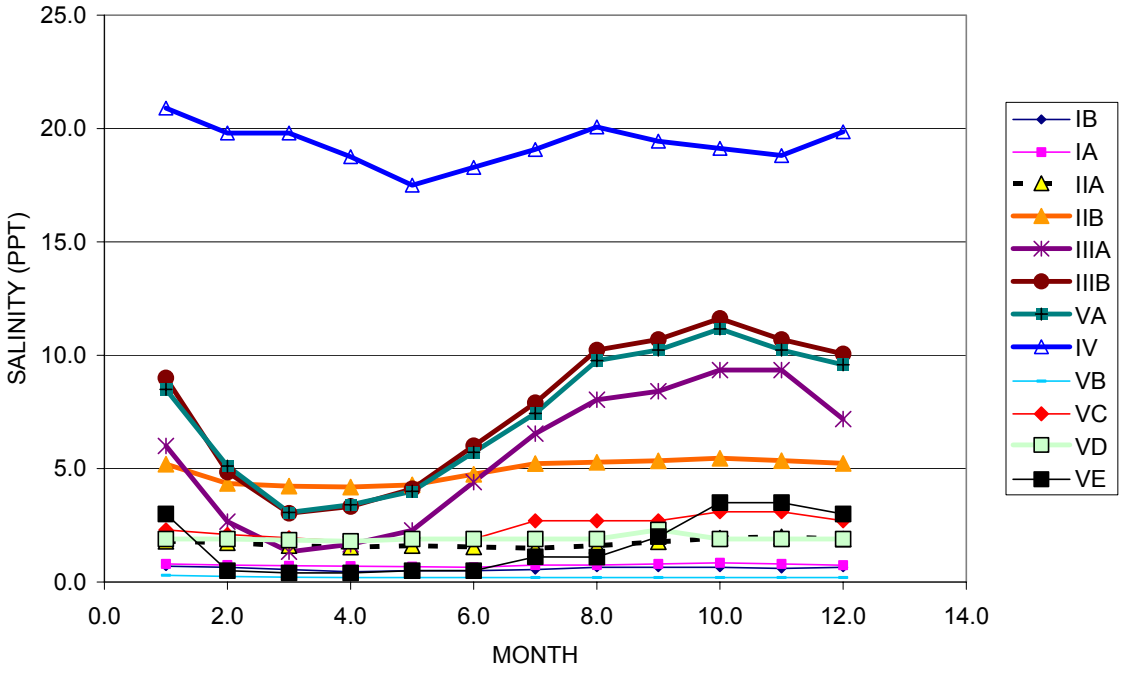

(stations are means for boxes as identified in Figure C.3-1)

Figure C.3-16 Monthly Mean Salinity for the Maintain Alternative, Subprovince 1

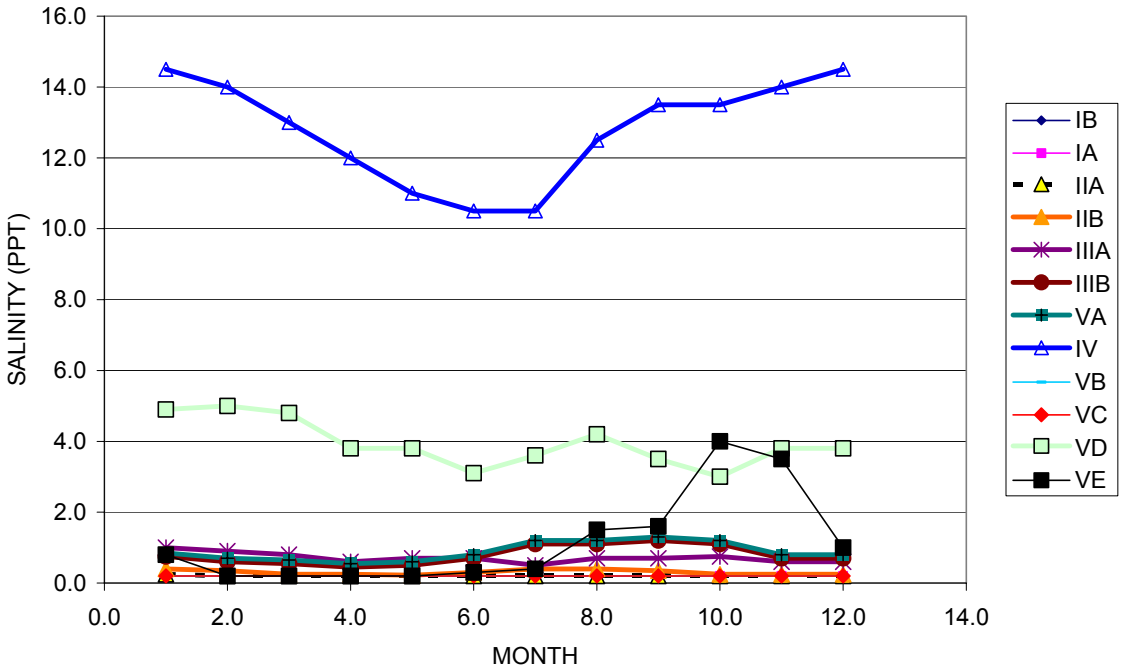

(stations are means for boxes as identified in Figure C.3-1)

Figure C.3-17 Monthly Mean Salinity for the Enhanced Alternative, Subprovince 1

3.8 Discussion of Model Limitations

Models are only approximations of reality and therefore all models are based on some assumptions and idealizations. The following list summarizes the notable assumptions in POM:

1. POM uses the hydrostatic assumption for pressure variation with depth.
2. The use of a sigma coordinate system requires that the variations in bed elevations be small. The model limitation is 20% bottom slope; however, even this may result in pressure gradient errors that affect the movement of external and internal waves. The large sigma gradients also affect the transport of mass in the system. This can lead to an underestimation of the saltwater intrusion into a shelf with steep bathymetry. For practical computation reasons the number of sigma layer was limited to 10 with surface and bottom refinement. A sensitivity study was conducted to determine that this was an adequate number of layers.
3. POM is limited to orthogonal grids. This makes it difficult to fit complex boundaries and narrow tributaries or passes. To accommodate this limitation it was necessary to adjust the depth and/or the roughness in some passes or channels to ensure that the hydraulic capacity is well represented. This leads to local errors in the solution in and near these elements.
4. All models should be validated. The POM used in this study has not been fully validated. The POM bathymetry was almost doubled to include the area between the mouth of the Mississippi and Gulfport by adding bathymetry from other working models. However,

data was only available for validation for the Lake Pontchartrain area. Time was not available to validate this model in the expanded domain; Inter-model comparisons have been made with the depth-averaged solutions obtained by RMA2/RMA4. There is general agreement of the depth-averaged circulation patterns and the salinity distribution. Figure C.3-9 shows a validation result for the POM model on Lake Pontchartrain stages.

5. All model are subject to uncertainty. Based on comparisons with a typical (10-year average) salinity distribution in the Pontchartrain Estuary, POM had an annual error in salinity of the order of +/- 1 ppt in the upper and middle regions and +/- 2 ppt in the lower regions or about 25% uncertainty. The relative predictions for the different scenarios with respect to the base were subject to similar uncertainty. Nevertheless, the final calibrated model appeared to predict the direction of any trend.
6. The POM was used to make a rough estimate of the distribution of dissolved inorganic nitrogen (DIN) in the plumes of the diverted Mississippi River water. These plumes were consistent with the zones of Lake Pontchartrain where historical algal blooms have been observed after the opening of the Bonnet Carré Spillway. The DIN submodel was calibrated with the 1997 Bonnet Carré data.
7. Georgiou (2002) conducted sensitivity studies on bed roughness in POM for Lake Pontchartrain. The bed roughness of 2 cm that was used in this study was based on this sensitivity analysis. Local adjustments in roughness were made to avoid unrealistic heads in evaluating large diversions.
8. POM does not have an explicit wetting and drying algorithm. The flooding of marshes was simulated by slightly lowering the marsh and compensating for this by increasing the frictional resistance. Flooding was based on the depth above the original marsh. This is an aspect of the model that needs improvement.
9. POM was very sensitive to ‘spikes’ in wind velocity. This problem was avoided by using 6-hour magnitude and direction-averaged wind inputs.
10. There are residual errors due to the assumed initial conditions. Due to the long hydraulic detention time of several months depending on the tributary flows in the Pontchartrain Estuary, the initial conditions for a one-year simulation can influence the solution for several months. This was partially corrected by using the December results for some trial runs as ICs for the final runs; nevertheless, this did have an influence on the predictions of some scenarios where there was a carry-over from the diversions of one year to the starting conditions for the next year. A simple cell model was used as an aid to improve the initial conditions for the three scenarios.
11. POM is generally 2^{nd} order accurate. It has an explicit external model for the gravity wave component. The second order scheme often produces unrealistic oscillation in the free surface and the transported variables. This can be overcome by upwinding; however, the use some schemes such as the 5-node 1st order upwind schemes introduces artificial diffusion. This can mask the real diffusion. These schemes can be combined with anti-diffusivity terms to over-come the stability or oscillation problems with adding excessive artificial diffusion. The temperature and salinity in the POM were run by a 2^{nd} order scheme. Some ‘rippling’ and ‘cluster’ instabilities were noted in the results if the time step was increased beyond a critical limit, and an additional complication was that the time step limit was strongly dependent on the wind shear.